JET–P(98)79

H-Y Guo et al

Edge Transport Barrier in JET Hot-ion H-modes

JET–P(98)79

Edge Transport Barrier in JET Hot-ion H-modes

H Y Guo, V Parail, P Andrew, B Balet, G D Conway, B de Esch, C Gowers, M von Hellermann, G Huysmans, T T C Jones, M Keilhacker, R König, P Lomas, A Maas, F Marcus, G F Matthews, F Nave[1], F Rimini, R Smith, M Stamp, A Taroni, P Thomas, K-D Zastrow.

JET Joint Undertaking, Abingdon, Oxfordshire, OX14 3EA,
[1]Associaçáo Euratom/IST, Lisbon, Portugal.

Preprint of a Paper to be submitted for publication in Nuclear Fusion

February 1999

ABSTRACT

The isotopic effects on the edge transport barrier are investigated for the ELM-free hot-ion H-mode discharges from the recent D-T experiments on JET. The role of fast particles is most clearly illustrated by comparing the pressure at the top of the edge transport barrier for the discharges with deuterium and tritium fast particle sources. The scaling of the experimental data from the D-D and D-T hot-ion H-modes supports the hypothesis that the width of the edge transport barrier can be controlled by the orbit losses of fast ions with a sufficient concentration in the edge. Based on this width scaling, the neoclassical theory predicts that the power losses through the separatrix scale as $P_{loss} \propto {n_{edge}}^2 Z_{eff,edge} {I_p}^{-1}$. It has now been demonstrated that this is consistent with the experimental data from the MkI and MkII divertors. However, a systematic increase in the loss power has been observed between the two divertor campaigns. A connection is proposed between this observation and the changes in the impurity production between the MkI and MkII divertors. The role of gas puff and edge recycling is also investigated.

1. INTRODUCTION

The hot-ion ELM-free H-mode discharges have delivered the world record for fusion power (16.1MW) [1] and have clearly demonstrated alpha particle heating [2] during the recent D-T experiments (DTE1) on JET. The characteristic feature of this regime is a low initial (target) plasma density, coupled with low levels of neutral recycling. The low target density, in combination with high power neutral beam heating allows the ions to be decoupled from the electrons and thus maximises fusion performance. Low levels of recycling as well as highly shaped plasmas and high plasma current are necessary to maximise both the ELM-free period and the fusion performance [3,4].

A key feature of the hot-ion H-mode lies in its edge transport barrier. The edge transport barrier controls the energy losses through the separatrix. It has been observed that the confinement, normalised to the ELM-free H-mode scaling prediction (ITER 93-H), rises approximately linearly with time, during the ELM-free phase, up to a factor ~ 1.8 [5] in the hot-ion H-mode plasmas. This observation has been explained in [5,6] by a model which requires the anomalous heat transport across the edge transport barrier region to be significantly reduced or suppressed so that the remaining transport approaches the level of ion neoclassical thermal conductivity. In addition, the edge transport barrier controls the edge ballooning and kink instabilities which are driven by the edge pressure gradient (ballooning mode directly and kink mode via bootstrap current). Assuming that the pressure gradient within the edge transport barrier is constant, both energy flux through the separatrix and the maximum plasma pressure at the top of the barrier are controlled by the width of the edge transport barrier. There are a variety of theoretical proposals about the possible scaling for the width of the edge transport barrier since the discovery of the

H-modes [5-15]. However, due to inadequate experimental information for the edge region which exhibits steep gradients, it is still not clear which mechanisms control the width of the edge transport barrier. Recently, it has been suggested that in some cases the width of the edge transport barrier can be controlled by the orbit losses of fast ions from neutral beam (NB) injection [16].

The significance of edge recycling and impurity production for the hot-ion H-modes is that the neoclassical model [5] predicts that the loss power through the separatrix is given by $P_{loss} \propto {n_{edge}}^2 Z_{eff,edge}$, with the assumption that the width of the edge transport barrier is given by the ion poloidal banana width $\Delta_{bar} \propto \sqrt{\varepsilon}\rho_{\theta i}$ with $\rho_{\theta i}$ being the Larmor radius of either thermal or fast ions. In going from the MkI to the MkII divertor, the loss power was increased significantly. The MkII divertor was designed with a more closed geometry compared to its MkI predecessor, as shown in Fig. 1, to reduce the flow of neutrals back into the confined plasma. It was thereby hoped to reduce the loss power by charge exchange in the edge plasma and to reduce the impurity production by the neutrals in the main chamber. In fact the neutral pressure in the MkII divertor is increased by about a factor of two, resulting in an significant increase in pumping [4]. However, one unexpected result of the MkII operation is that the impurity production yield at the target is about a factor of two higher in the MkII divertor than that in MkI, which is attributed to the enhanced chemical sputtering in MkII due to the higher base temperature of the MkII divertor target plate [17].

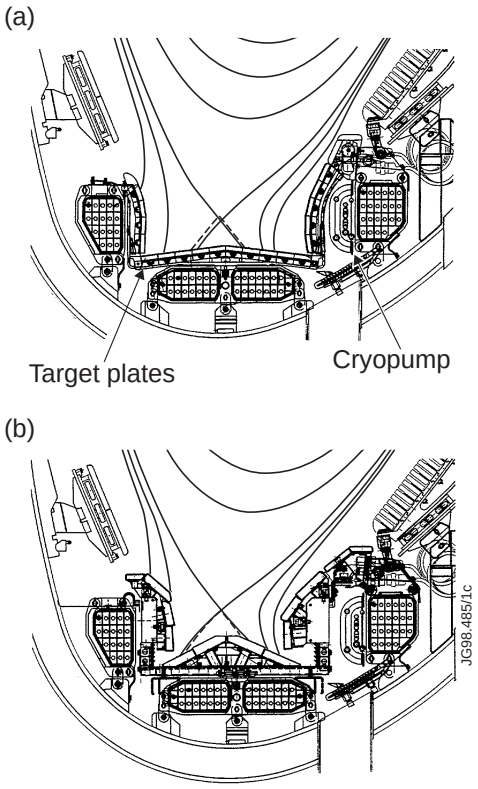

Fig. 1. Poloidal cross sections of the JET MkI (a) and MkII (b) divertors.

The outline of the present paper is as follows. In Section 2 we report the experimental observations of the isotopic effects on the edge transport barrier in the hot-ion H-modes from the DTE1 campaign and show the detailed evidence for the role of fast particles. In Section 3 we first describe the models for the width of the edge transport barrier, followed by the experimental scaling of the edge transport barrier width with different model assumptions. In Section 4 the loss power is compared with the predictions from the neoclassical transport model, based on the width scaling for the edge transport barrier. In Section 5 we attempt to explain the difference in loss power between the MkI and MkII divertors in terms of the neoclassical heat transport within the edge transport barrier and hence demonstrate the significance of the edge recycling and the impurity production for the hot-ion regimes. The summary and conclusions follow in Section 6.

2. ISOTOPIC EFFECTS ON EDGE TRANSPORT BARRIER

2.1. Edge pressure and ELM free period in D-D and D-T

While it is affected by a variety of MHD phenomena, such as the sawteeth or the outer modes [18], the performance phase of the hot-ion H-mode is eventually terminated by the occurrence of a giant Type I ELM [19]. It has been shown that the Type I ELM [20] is usually associated with the ideal ballooning modes [21]. This is consistent with the observations of the hot-ion modes at different plasma currents, which shows that the giant (Type I) ELM occurs as the edge pressure gradient approaches the ballooning instability limit [22].

At JET the edge pressure, including both electron and ion pressure, i.e., $p_{edge} = (n_e T_e + n_i T_i)_{edge}$, is measured at R = 3.75 m, corresponding to $r/a \approx 0.9$, at the top of the pedestal, inside the steep gradient region. The edge electron density, n_{edge}, is a line average, determined by the edge channel of the interferometer. The edge electron temperature, $T_{e,edge}$, is a local measurement at the same position, obtained from the Electron Cyclotron Emission (ECE). The ion pressure at the edge is measured by the Charge eXchange (CX) diagnostics taking into account impurity dilution. Fig. 2 shows the evolution of the edge pressure (P_{edge}), together with the other plasma parameters at the edge for a hot-ion H-mode in D-D (#41068), in comparison with that in D-T with ~60% tritium in the discharge(#42856). Both pulses have the same plasma current (3.8MA) and toroidal magnetic field (3.4T). The total heating power supplied by the Neutral Beams (NB) is also the same (~ 10MW), but for the D-T pulse the neutral beams consists of the same isotopic composition as in the plasma. In addition, up to 2MW of ICRF heating is applied in the D-D pulse to simulate the alpha heating which would occur in D-T. As can be seen in Fig. 2, after the initial threshold ELMs the edge pressure grows with time at the same rate for both the D-D and D-T pulses. However, the D-T discharge proceeds further and reaches a higher edge pressure at the onset of the giant ELM, hence explaining the longer ELM-free period, as indicated by the $D\alpha$ emissions from the divertor. The evolution of the electron density (n_{edge}), the electron temperature ($T_{e,\,edge}$) and the ion temperature ($T_{i,\,edge}$) at the edge in D-T is also reproduced by the D-D alpha simulation pulse.

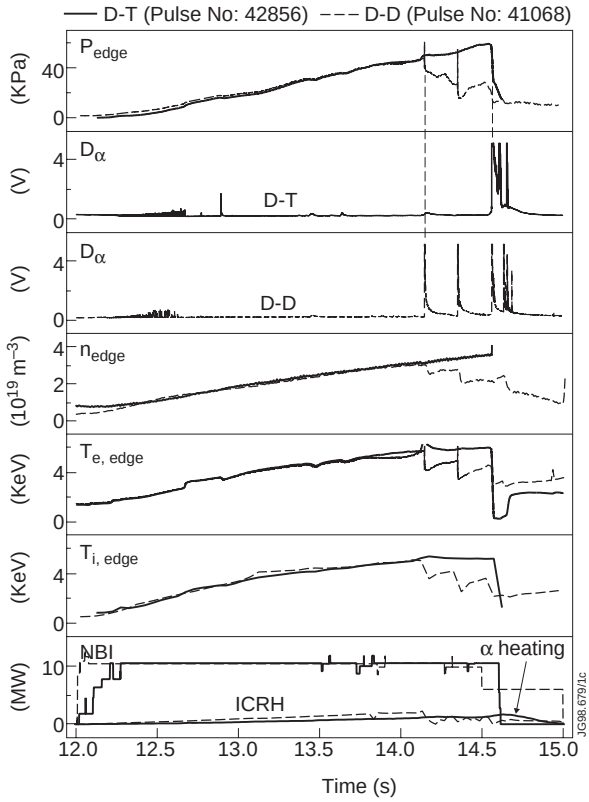

Fig. 2. Time traces of two comparable hot-ion H-modes (10MW, 3.8MA, 3.4T) performed in D-D (#41068) and in D-T (#42856) illustrating the changes in the edge pressures. Data shown are the edge pressure, $D\alpha$ emissions from the strike zone in the outer divertor, the electron density, the electron temperature, the ion temperature, as well as the additional heating power.

Note that comparing D-D and D-T discharges at the same beam power, but without simulating the effect of alpha heating, shows that the rise of the edge pressure in D-D is generally slower than that in D-T. This results in the ELM-free periods as long as the D-T cases. However, it is possible that this arises from differences in recycling, according to how the walls were pre-loaded with D-T. To investigate the effect of recycling, independent of isotopic effects, Fig. 3 compares the evolution of the edge parameters for two D-D discharges with different recycling levels. The two discharges have the same NB heating power as the discharges shown in Fig. 2. As can be seen, at higher recycling level, the edge density rises faster, but the rise in both electron and ion temperatures at the edge is reduced. As a result, the evolution of the edge pressure is similar for the two discharges, reaching similar edge pressure values at the onset of the giant ELM. Notice that the maximum pressures obtained in these two discharges are comparable to that in the D-D alpha particle simulation discharge (with ICRH) (Fig. 2) in spite of very different recycling conditions. The ELM-free periods in the NB only D-D discharges are longer due to the slower rate of rise in edge pressure, compared to the alpha particle simulation pulse.

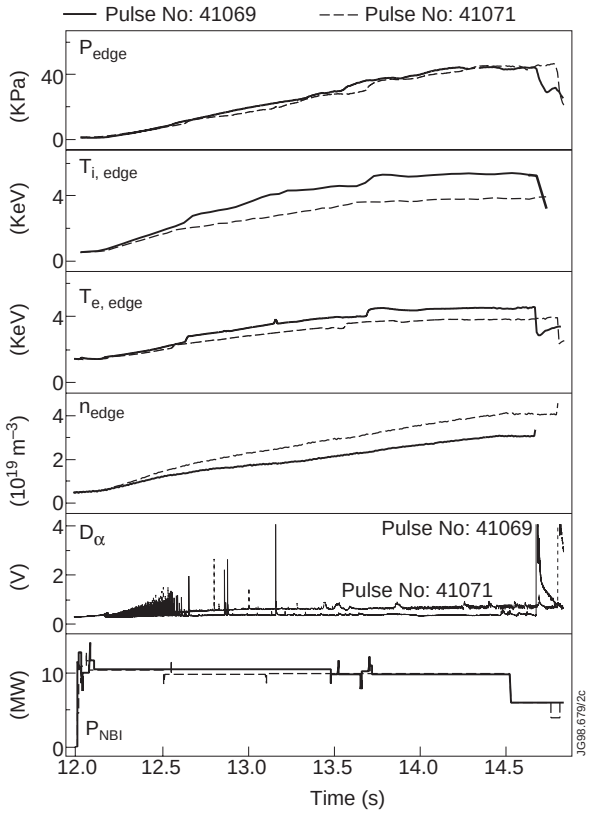

Fig. 3. Evolution of the edge pressure, the ion temperature, the electron temperature and the electron density of two D-D hot-ion H-modes with the same neutral beam heating (10MW), but with different recycling conditions.

A large number of the D-D discharges with different edge recycling conditions were carried out prior to the D-T campaign. It is found that with similar plasma current and additional heating, the maximum edge pressure in D-D is lower than that obtained in D-T. Assuming that the type I (giant) ELMs occur at the same critical pressure gradient and that this is dictated by the ballooning instability suggests that the width of the edge transport barrier is larger in D-T than that in the D-D discharges, as will be further discussed in the following sections.

It is well known that the hot-ion H-mode plasma is very rich in the different type of MHD phenomena such as sawteeth and outer modes [19], which might sometimes interfere with ELMs and thus affect both the edge pressure and the ELM-free period. The simplest example is a sawtooth crash which redistributes the plasma pressure and can lead to a sudden increase in the edge pressure followed by a prompt ELM. Since our assumption is that the cause of Type I ELM is the ballooning instability, the edge pressure should be measured as close to the onset of the

ELM as possible. The outer modes (driven by the external ideal kink instability [18]), like ELMs, are also edge localised phenomena. If they are localised in the plasma inside the edge transport barrier, we might expect an increase of the edge pressure, which should be taken into account while evaluating the edge pressure. However, we sometimes observe a decrease in the edge pressure due to the outer modes. This might happen in a case where the outer modes are localised within the barrier outside the position of our edge measurements (at r/a ≈ 0.9). Such outer modes could cause a local perturbation of the pressure gradient within the barrier region, and hence trigger a relatively small ELM. In this case our measurements are not reliable and are therefore excluded from analysis. In addition, some small benign ELMs could occur before the edge pressure reaches a critical level. There are a number of phenomena which might case these "premature" ELMs, such as UFOs. In the present paper, we will not discuss these small ELMs and concentrate on the giant ELM which destroys the edge transport barrier and terminates the high performance phase of the hot-ion H-modes.

2.2. Effect of fast particles

To investigate systematically the isotopic dependence of the width of the edge transport barrier, we have chosen a series of discharges during the alpha particle heating experiments, described in [2]. These discharges were performed at 3.8MA/3.4T with constant neutral beam heating power (10 MW) and little variation in the particle source. The tritium concentration in the plasma was varied from 0 to 100% by simultaneous control of the fuelling from neutral gas and from the neutral beam injection system. The vacuum vessel walls and divertor target were also loaded with the required DT mixture to ensure that the recycling composition was as close to that of the gas and NBI sources as possible.

Fig. 4 shows the critical edge pressure at the onset of the giant ELM (which terminates the high fusion performance phase), as a function of the edge isotopic composition. The tritium concentration, $n_T/(n_T + n_D)$ is determined from a high resolution visible spectrometer, which measures the recycling composition and is representative of tritium concentration near the edge. The critical edge pressure appears to be higher in the tritium rich discharges. A few deuterium reference discharges for the alpha particle heating experiments are also shown. A survey of the entire 10 MW hot-ion H-mode data base shows that no other deuterium discharges reach a critical edge pressure above the data shown in Fig. 4 for the D-D pulses. From this it cannot be deduced whether the higher edge pressure in D-T is due to fast or thermal ions since the isotopic composition of the NBIbeam particle source is similar to that in the background plasma. This is however clarified by results from the discharges with pure deuterium background plasma but 25%, 60% and 100%, respectively, tritium neutral beams, also shown in Fig. 4. The edge pressures in the discharges with 60% and 100% tritium beams are higher than the D-D discharges and comparable to other tritium rich discharges. This strongly suggests that the edge transport barrier width is determined by the fast particles.

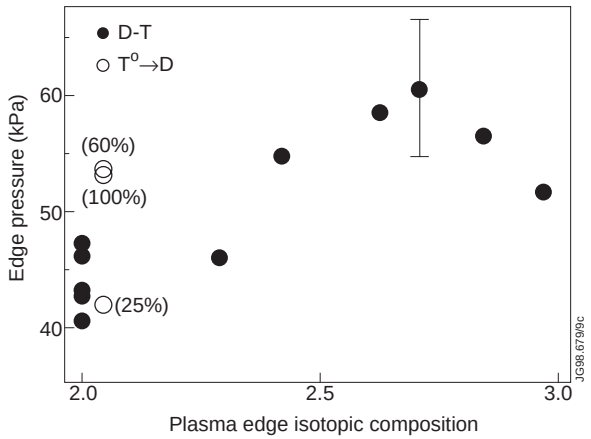

Fig. 4. Edge pressure at the onset of ELMs vs. edge isotopic composition for a series of 3.8MA/3.4T hot-ion H-modes with NBI power of ~10 MW, in which the isotopic composition of the NBI beam particle source is closely matched to that in the background plasma. In addition, the data from discharges with a pure deuterium background plasma and tritium fast particles from the neutral beams are shown for comparison.

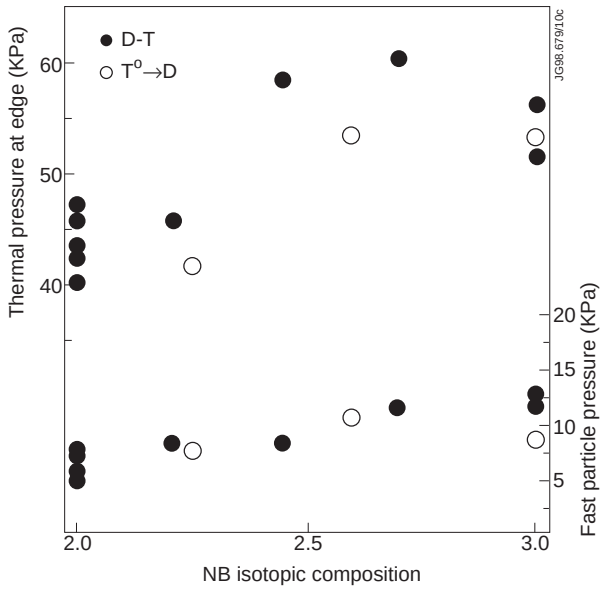

Fig. 5. Edge pressure at the onset of ELMs vs. the isotopic composition of the neutral beams. The fast particle pressure at the edge is also shown.

To further illustrate the effect of fast particles, Fig. 5 plots the edge pressure versus the isotopic composition in the neutral beams. In the figure is also shown the fast particle pressure computed with the self-consistent beam deposition code CHEAP (CHarge Exchange Analysis Package) [23], which is benchmarked by computations with the TRANSP code. As can be seen, the discharges with higher tritium beam composition have a higher edge pressure than the discharges with only deuterium beams. In addition, the fast particle pressure also tends to increase with the tritium concentration in the beams. However, with low tritium beam concentration, the edge pressure is reduced to the level similar to the deuterium only discharges. This might suggest that the fast particle concentration at the edge should exceed a certain level in order to be sufficient for the control of the edge transport barrier. This result is consistent with the idea [16] that the concentration of fast particles should exceed a certain level (about 1% of the thermal ion density) in order for them to play a decisive role in the determination of the radial electric field, which in turn controls the transport barrier width. The detailed information on the edge parameters at the onset of the giant ELMs for the discharges shown in Fig. 4 and Fig. 5 are listed in Table I.

Further evidence for the fast particle effect is shown in Fig. 6, where two deuterium-only discharges at 3.8MA/3.4T are compared. Both have similar NBI heating power, ~ 10 MW, but in #42612 about 8 MW of the high energy (140KeV) beams are substituted for the lower energy (80KeV) beams. Therefore, the fast particle energy, $\langle E_{fast} \rangle$, is lower in #42612 than #42590, as shown in Fig. 6, where $\langle E_{fast} \rangle$ is the averaged energy of the fast particles which are present in

Table I Parameters of interest for a series of low power heated 3.8MA/3.4T hot-ion H-modes with different tritium mix in the edge plasma and in the neutral beams, including: (a) deuterium only discharges with different recycling conditions, (b) discharges with deuterium background plasma and fast tritium sources from the neutral beams; and (c) discharges with similar tritium mix in both the edge plasma and the beams. In particular, in the table are also listed the discharges with additional ICRH to simulate the alpha particle heating which would occur in D-T.

Pulse No.	T/(D+T) (Edge)	T/(D+T) (Beams)	P_{NBI} (MW)	P_{ICRF} (MW)	P_{α} (MW)	$n_{e,edge}$ (10^{19} m^{-3})	$T_{e,edge}$ (KeV)	$T_{i,edge}$ (KeV)	$Z_{eff,edge}$	p_{edge} (KPa)
41069	0	0	6.0	0	0	3.07	4.53	5.22	2.20	42.99
44401	0	0	10.8	0	0	3.74	3.90	3.88	2.10	40.49
42578	0	0	10.6	0	0	3.75	3.90	3.90	1.86	42.75
41071	0	0	6.0	0	0	4.07	3.94	3.92	2.11	46.12
41067	0	0	10.6	0.87	0	3.06	4.81	5.31	2.31	43.28
41068	0	0	10.4	1.97	0	3.02	5.79	5.0	2.20	47.21
42647	4%	25%	10.9	0	0.58	3.92	3.92	3.83	2.17	42.03
42657	5%	60%	10.1	0	0.97	4.03	4.82	4.36	1.97	53.49
42656	5%	100%	8.3	0	0.91	3.98	4.87	4.05	1.72	53.32
42870	29%	21%	10.1	0	0.75	3.23	4.22	4.65	2.28	46.0
42856	63%	45%	10.5	0	1.40	3.60	5.81	5.21	2.39	58.59
42847	71%	70%	10.2	0	1.50	3.79	5.46	5.40	2.17	60.48
42840	84%	100%	10.6	0	0.77	3.63	5.50	5.33	2.55	55.54
43011	97%	100%	10.5	0	0.30	4.21	4.80	4.14	2.97	51.18

the edge, obtained from CHEAP analysis. The evolution of the electron pressure at the edge, $P_{e,edge}$, is similar for the two discharges. However, the discharge with higher fast particle energy proceeds further and reaches a higher edge pressure at the onset of the giant ELM. Notice that the ion temperature ($T_{i,edge}$) at the onset of the giant ELM is about the same for the two pulses.

Additional evidence of the fast particle effects comes from the results obtained from the steady state ELMy H-modes [24]. In particular, the influence of the fast particle component at the edge on the ELM behaviour is demonstrated in RF heated discharges where the deposition profile of the fast particles was shifted to the edge by applying part of the heating power to the edge [24].

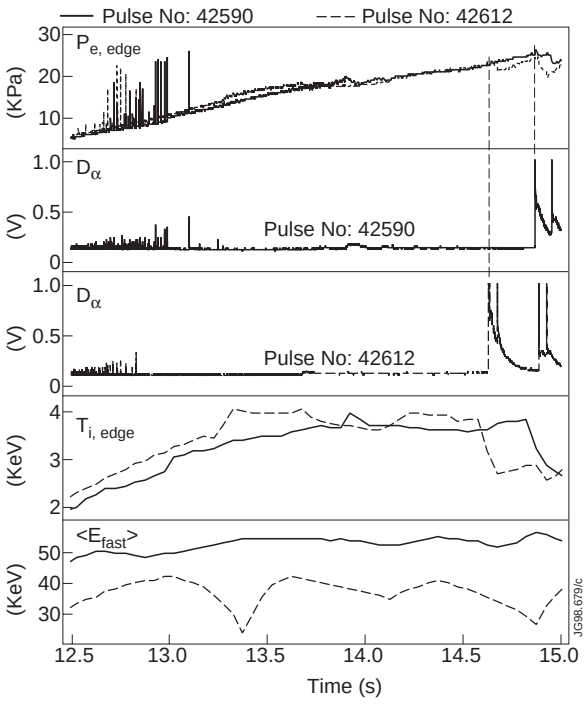

Fig. 6. Time traces of two comparable pure deuterium discharges, #42590 and #42612. Both discharges have similar NBI heating (~10MW), but high energy beams dominate in #42590.

3. EDGE TRANSPORT BARRIER WIDTH

3.1. Models

Different models for the width of the edge transport barrier have been proposed since the discovery of the H-mode. The oldest one, which is related to the turbulence stabilisation by an externally imposed radial electric field [7], assumes that the width of the edge transport barrier (Δ_{bar}) is controlled by the ion orbit losses. It implies that the barrier width, $\Delta_{bar} \propto \sqrt{\varepsilon} \cdot \rho_{\theta i}$ with $\rho_{\theta i}$ being the poloidal ion Larmor radius. It was assumed in [5] that the transport barrier width is controlled by the losses of the thermal ions. However, it was found that Δ_{bar} should be a few (3 to 5) ion banana orbit radii in order to match the pressure at the top of the edge transport barrier with Ballooning stability criteria [25].

Another idea, which was discussed recently, is that the transport barrier width is controlled by the radial correlation length of the turbulence itself [8-11]. This idea is actually two fold. Firstly the radial correlation length is a reasonable measure for the turbulence suppression length by itself. Secondly the radial correlation length is a good measure of the radial electric field width which is self-induced by a nonlinear wave cascading. Three different expressions for the radial correlation length have been proposed: $\Delta_{cor} \approx \rho_i \propto \rho_{\theta i}$[5]; $\Delta_{cor} \approx \sqrt{\rho_i a}$ [9,10]; and $\Delta_{cor} \approx \sqrt[3]{\rho_i{}^2 a}$ [11]

The next concept is the idea of the turbulence suppression by the finite ion Larmor radius [12-14]. We can expect this mechanism to be effective in suppressing the short wavelength turbulence with the characteristic radial correlation length of the order of the ion Larmor radius.

It was also suggested that the width of the transport barrier could be controlled by the atomic physics processes such as the ionisation of cold neutrals [15]. The physics behind this idea is that neutrals can act as an agent which takes the momentum from the ions and in this way control the shear in the plasma rotation. If this is the case, we might expect the width of the transport barrier to scale as: $\Delta_{bar} \approx \sqrt{V_{Ti}^2 / n_e^2 \cdot \langle \sigma v_e \rangle_{ion} \cdot \langle \sigma v \rangle_{cx}}$ where $n_e \cdot \langle \sigma v_e \rangle_{ion}$ is the rate of the cold neutral ionisation and $n_e \cdot \langle \sigma v \rangle_{cx}$ is the rate of the charge exchange between neutrals and ions.

The new experimental evidence from the JET hot-ion H-modes (Section 2.2) shows that in some situations the transport barrier width could be controlled by the fast particles provided by the neutral beams. Assuming that the width of the transport barrier is controlled by the orbit losses of fast particles gives: $\Delta_{bar} \approx \sqrt{\varepsilon} \cdot \rho_{\theta i}^{fast}$. For a typical 3.8MA/3.4T hot-ion plasma, $\Delta_{bar} \propto \sqrt{\varepsilon}\rho_{\theta i} \approx 0.63\sqrt{T(KeV)}$. With a fast particle energy of 70 KeV (typical in the hot-ion H-modes), the transport barrier width is estimated to be about 5 cm, which is consistent with the experimental measurements [26].

3.2. Scaling of the barrier width

The direct determination of the edge transport barrier width requires simultaneous detailed measurements of electron density, electron temperature, ion temperature and the Z_{eff} profiles. This

has proven very difficult on JET due to the steep gradients at the edge and inadequate spatial resolution of the diagnostics for this purpose [26]. As an alternative approach we adopt a simplified method [10], based on the assumption that the onset of the type I ELMs is controlled by the ballooning stability limit for the scaling of the edge barrier width using the measurements at the top of the edge pedestal (R=3.75 m, or r/a ~ 0.9).

Assuming that the giant (type I) ELMs are triggered by the edge ballooning instability, we can obtain the following expression for the critical pressure gradient [27]: $\nabla p^c \approx {p_{edge}}^c / \Delta_{bar} \propto {B_\phi}^2 / Rq^2 \cdot \varphi(s)$where B_ϕ is toroidal magnetic field and q is the safety factor. $\varphi(s)$ depends on the magnetic shear and other details of the magnetic configuration within the barrier. With the same magnetic configuration, the following simple relation for the critical edge pressure is obtained:

$$ {p_{edge}}^c \propto {I_p}^2 \cdot \Delta_{bar} $$

where I_p is plasma current.

If the width of the edge transport barrier is given by the poloidal Larmor radius of fast ions, i.e., $\Delta_{bar} \propto \sqrt{M_{fast}\langle E_{fast}\rangle} \cdot {I_p}^{-1}$, we then obtain:

$$ {p_{edge}}^c \propto \sqrt{M_{fast}\langle E_{fast}\rangle} \cdot I_p $$

Assuming the edge transport barrier is controlled by the poloidal Larmor radius of the thermal ions gives:

$$ {p_{edge}}^c \propto \sqrt{M_{eff} T_i} \cdot I_p $$

where M_{eff} is the effective mass of the D-T isotopes at the edge.

Fig. 7 plots the experimental data against the fast particle scaling, i.e., ${p_{edge}}^c \propto \sqrt{M_{fast}\langle E_{fast}\rangle} \cdot I_p$, where M_{fast} and $\langle E_{fast}\rangle$ represents mass and averaged energy of D/T fast particles, together with the edge pressure values predicted by the ballooning instability limit with the assumption that $\Delta_{bar} = \sqrt{\varepsilon}\rho_{\theta i}{}^{fast}$. The database includes the 10 MW D-T discharges shown in Fig. 4, and also covers high power (up to 20MW) neutral beam heated discharges, as well as both low power and high power combined NB and ICRF heated discharges. The plasma current within the data set varies from $I_p = 1.5 - 4.0 MA$. The magnetic configuration for these discharges are the same, with the magnetic shear around 3.6 at 95% magnetic flux surface. It appears that there is a rather good correlation between the edge pressure and the fast ion Larmor radius, except in the discharge with lower tritium beam concentration (25%) where the tritium fast particle concentration seems to be insufficient to affect the barrier width, as discussed in Section 2.2. In fact, the scaling with the deuterium fast particle Larmor radius renders it in line with other data (not shown). The experimental data not only show the trend of the scaling of the Larmor radius of fast particles, but also have similar magnitudes compared to

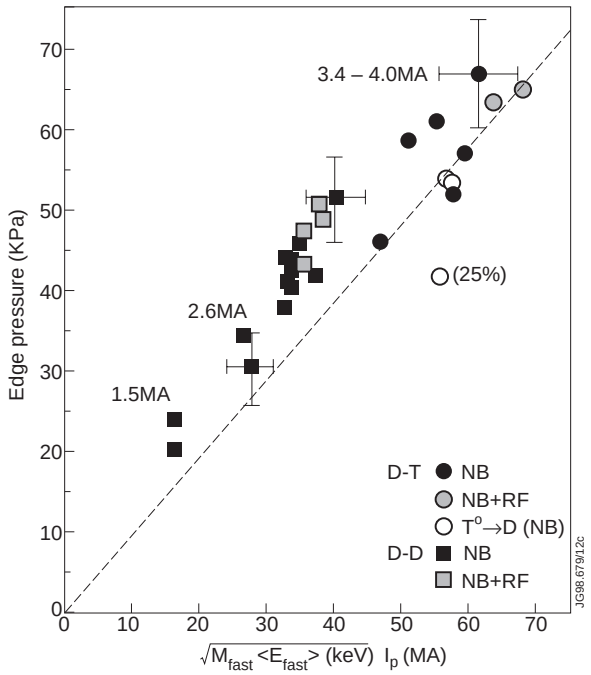

Fig. 7. Scaling of the edge transport barrier width with the Larmor radius of the fast particles for D-D and D-T ELM-free hot-ion H-modes including both low power and high power NB and combined heating (NB+ICRF) discharges. The experimental data are taken at the onset of the giant ELM which terminates the high fusion performance. The dashed line indicates the edge pressure values expected from the ballooning instability limit with $\Delta_{bar} = \sqrt{\varepsilon}\rho_{\theta i}{}^{fast}$.

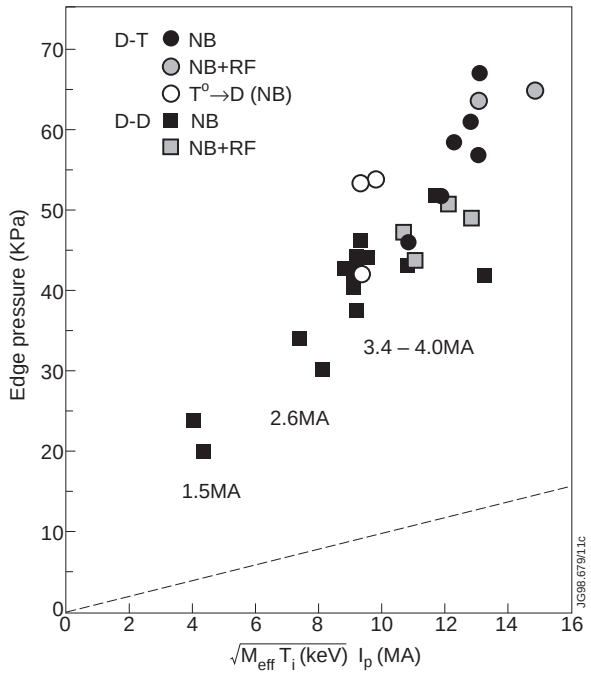

Fig. 8. Scaling of the edge transport barrier width with the Larmor radius of the thermal ions for D-D and D-T ELM-free hot-ion H-modes. The dashed line indicates the edge pressure values expected from the ballooning instability limit with $\Delta_{bar} = \sqrt{\varepsilon}\rho_{\theta i}{}^{th}$.

the estimate of the edge pressure values from the ballooning instability limit. It is worth while to mention that the scaling shows a clear I_p dependence of the edge pressure, which further confirms the dependence upon $\rho_{\theta i}$.

For comparison, Fig. 8 shows the results with the assumption that the transport barrier width is proportional to the Larmor radius of thermal ions, together with the model estimate of the edge pressure values with $\Delta_{bar} = \sqrt{\varepsilon}\rho_{\theta i}{}^{th}$. It appears that the strong I_p dependence remains, but there is no clear trend with $\sqrt{M_{eff}T_i}$ at similar plasma currents (3.4-4MA). In addition, the experimental edge pressures are much higher than the expectations from the ballooning instability limit, as shown in the figure. The scaling of the edge pressure produces similar scatter assuming the different dependence upon the thermal ion Larmor radius, i.e., $\Delta_{bar} \approx \sqrt{\rho_{i,th}a}$ or $\Delta_{bar} \approx \sqrt[3]{\rho_{i,th}{}^2 a}$, which are predicted by the other models, as described in Section 3.1. In contrast, the model based on the atomic physics processes predicts lower pedestal pressure for the D-T plasmas since the recycling tritium neutrals would penetrate less deeply into the plasma before ionisation compared to deuterium neutrals, contrary to the experimental observations.

4. LOSS POWER THROUGH THE TRANSPORT BARRIER

4.1. Neoclassical losses

Two main mechanisms of heat loss from the barrier region have been identified in Hot-ion H-modes. The first one is related to the diffusive losses through the transport barrier and the separatrix. The second one is attributed to the non diffusive losses of the hot-ions via their charge exchange with the cold neutrals and subsequent escape from the confinement zone.

The diffusive losses are caused by the finite ion and electron thermal conductivity within the transport barrier. It was proposed in [5,6] that the anomalous ion transport within the transport barrier is completely suppressed in the Hot-ion H-mode so that ion heat flux is provided by the ion neoclassical thermal conductivity:

$$q_i \approx -n_i \chi_i^{neocl} \nabla T_i \tag{1}$$

Since the edge transport barrier is quite narrow ($\Delta_{bar}/a << 1$) we can make the following substitution: $n_i \nabla T_i \approx -(n_i T_i)_{edge}/\Delta_{bar}$ which gives instead of Eqn. (1):

$$q_i \approx (n_i \chi_i^{neocl} T_i)_{edge}/\Delta_{bar} \tag{2}$$

It was assumed [7] that close to the separatrix (within the distance of the ion poloidal Larmor radius), the ion conductive neoclassical heat flux is converted into the convective flux produced by the direct ion losses. To ensure plasma ambipolarity we can assume that either the electron anomalous transport is reduced to the level of the ion neoclassical transport, i.e., $\chi_i \approx \chi_e \approx D \approx \chi_i^{neo}$ [5,6,25], or the direct ion losses are compensated by the influx of cold ions from outside the separatrix [7]. In the latter case the losses through the electron channel should be significantly reduced with respect to the corresponding losses through the ion channel ($q_e << q_i$). Due to limited experimental information, we cannot discriminate between these two cases at present.

For the non diffusive channel of the energy losses - charge exchange between hot-ions and cold neutrals, we can estimate the maximum charge exchange heat flux assuming 100% recycling from the wall. In this case the influx of cold neutrals should be equal to the outgoing flux of the ions. With the neo-classical transport barrier, the following expression for the particle flux through the separatrix can be obtained:

$$\Gamma \propto q_i / T_{i,edge} \approx (n_i \chi_i^{neocl})_{edge}/\Delta_{bar} \tag{3}$$

where $T_{i,edge}$ is the ion temperature at the top of the transport barrier. To find the characteristic heat flux produced by the charge exchange losses we should multiply Eqn. (3) by the characteristic ion temperature within the region of the most intensive charge exchange interaction. The numerical analysis [5] shows that this region is localised inside the transport barrier. Therefore,

the charge exchange losses are qualitatively similar to the neoclassical losses through the transport barrier ($q_{cx} \sim q_i$) but could have a slightly larger magnitude.

It follows from the above analysis that the total heat flux through the separatrix (loss power): $P_{loss}{}^{ccx} \approx q_i + q_e + q_{cx} \propto q_i$, which is given by Eqn. (2). Assuming that Δ_{bar} is controlled by the Larmor radius of the fast ions, we obtain the following expression for the loss power:

$$P_{loss}{}^{ccx} \propto n_{edge}{}^2 Z_{eff,edge} I_p{}^{-1} \sqrt{T_i / \langle E_{fast} \rangle}$$

provided that the fast ions have the same isotopic composition as the thermal plasma ions. $\langle E_{fast} \rangle$ is the average energy of fast particles including both deuterium and tritium fast ions. n_{edge} and $Z_{eff,edge}$ are the density and Z_{eff} at the edge respectively. Alternatively, with an assumption that Δ_{bar} is controlled by the Larmor radius of the thermal ions, we then obtain:

$$P_{loss}{}^{ccx} \propto n_{edge}{}^2 Z_{eff,edge} I_p{}^{-1}.$$

4.2. Loss power in D-D and D-T

The power loss through the separatrix is determined by subtracting the radiation inside the separatrix ($P_{rad,core}$) and the change in the content of thermal energy (dW_{th}/dt) from the total heating power absorbed by the thermal plasma ($P_{in}{}^{th}$), i.e., $P_{loss}{}^{ccx} = P_{in}{}^{th} - dW_{th}/dt - P_{rad,core}$, where $P_{in}{}^{th}$ is computed by TRANSP, including Ohmic heating, the total thermal heating from the ICRF and the neutral beams (taking account of orbit losses, beam shine through and charge exchange losses), as well as the heating of the thermal plasma by rotation friction. In addition, the heating from the alpha particles is included for the D-T discharges. W_{th} is also obtained from TRANSP analysis. $P_{rad,core}$ is measured by the bolometers.

Fig. 9 plots the loss power, $P_{loss}{}^{ccx}$, against the predictions from the neoclassical models for two of the best fusion performance hot-ion H-modes, i.e., #40346 and #42677, in MkII with the neutral beam heating only with $I_p = 3.8MA$ and $B_T = 3.4T$. #40346 is in pure D-D with ~ 19MW of NB heating, while the D-T discharge (~50%-50% D-T) has a higher fast particle energy from the tritium beams, and hence has higher neutral beam heating power (~23MW) with a larger population in the high energy beam box. The experimental data are taken from the ELM-free period in the discharges. It appears that there is a rather good

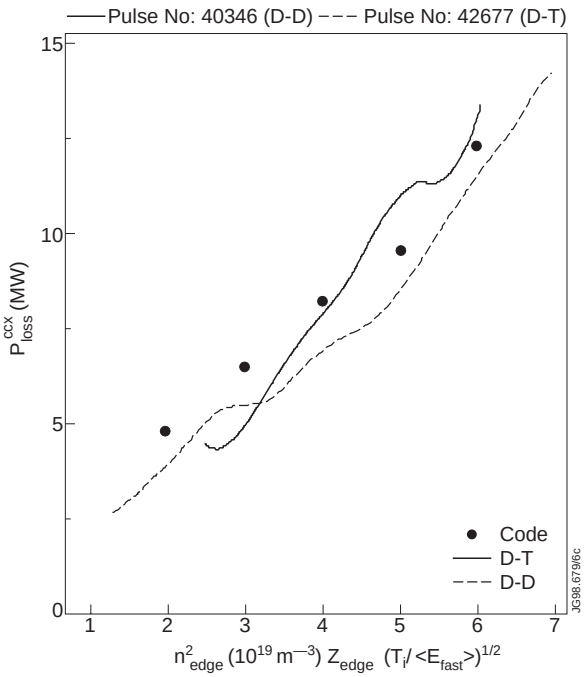

Fig. 9. P_{loss} from the D-D (#40346) and D-T (#42677) discharges against the predictions from the neoclassical models assuming the edge transport barrier width is proportional to the Larmor radius of fast particles, together with the predictions from the JETTO code.

correlation between $P_{loss}{}^{ccx}$ and $n_{edge}{}^{2} Z_{eff,edge} \sqrt{T_i / \langle E_{fast} \rangle}$ as predicted by the neoclassical model based on the assumption that the transport barrier width is proportional to the Larmor radius of fast ions. In addition, Fig. 9 shows the loss power calculated by the fully predictive JETTO code [5] for the D-T pulse, including the neoclassical and charge exchange losses, to compare with the experimental scaling. As can be seen, the code predicts not only the dependence of the power losses on the edge plasma parameters but also gives quantitative agreement with the experimental results. For this case, the charge exchange loss is about the same as the neoclassical losses.

Since D-T discharges appear to have a larger edge transport barrier width than that in D-D, we might expect that the energy content of D-T plasmas should rise faster because of the smaller neoclassical and charge exchange losses. Combining this with the better ballooning stability at the edge, we might therefore expect higher performance in a D-T plasma than in its D-D counterpart. In fact similar levels of performances are delivered in the D-D and D-T hot-ion modes. The detailed analysis of this surprising result must involve the core transport and lies outside the scope of this paper. Here we limit ourselves with some qualitative assessments. One possible explanation is as follows. If the core transport were controlled by a combination of a gyro-Bohm ($\chi_{gyro-Bohm} \propto \sqrt{m_i}$) and a Bohm type ($\chi_{Bohm} \propto m_i{}^{0}$) of turbulence as it was proposed in the JET model [5,6], then the transport in the central part of the plasma would be dominated by the $\chi_{gyro-Bohm}$, which is stronger in D-T mixture, offsetting the pedestal effect. This would thus degrade the core confinement. In addition, it is observed in the experiments that, in general, the edge density rises faster in D-T, which could therefore result in a faster increase in the edge losses. Apart from the core confinement degradation, the possible difference in the edge recycling between the deuterium and tritium neutrals could also be responsible for the higher edge density in D-T. In particular, the cold neutrals which are always present in the edge are much more localised near the separatrix in the case of a tritium plasma than a deuterium plasma, which might therefore lead to a relative increase in the edge plasma density in the T-enriched plasma. In addition, the tritium beams can produce broader power and particle deposition profiles than the deuterium neutral beams, but the TRANSP analysis shows that the differences are actually very small.

5. COMPARISON BETWEEN MKI AND MKII

5.1 Impurity behaviour

As demonstrated above, the power losses through the separatrix are explicitly dependent on the Z_{eff} at the edge. The impurity concentration within the edge transport barrier inside the separatrix is determined by the impurity sources and the transport of the impurities through the SOL. The divertor impurity sources in the MkI and MkII divertors, are compared in Fig. 10, where the average *CIII* photon flux is plotted against the D_α intensity from the outer strike zones for the

hot-ion H-modes during the ELM-free phase. As can be seen, the *CIII* intensity is about a factor of 2 higher in the MkII divertor than that in the MkI divertor for a given $D\alpha$ flux. The *CIII* and $D\alpha$ emissions from the inner divertor show similar results. It is to be noted that the electron temperature and density at the target plate are very similar for MkI and MkII hot-ion discharges at the strike points, as measured by the target Langmuir probes. Therefore, the higher *CIII*/$D\alpha$ ratio suggests an increased impurity production yield at the MkII divertor target. The best explanation for the higher yield is that the chemical sputtering yield is increased due to the higher target temperature of the MkII divertor[17]. Specific experiments with lower wall temperature in MkII support this explanation [28].

Contrary to the high recycling regime [29,30], the divertor/SOL screening for the impurities is poor in the low recycling hot-ion regime [17]. Consequently, the higher impurity flux produced in the MkII divertor results in a significant increase in the Z_{eff} at the edge, upstream from the target, compared to MkI, as illustrated in Fig. 11, where the measured Z_{eff} at the edge is plotted against the density at the edge for the pulses of Fig.10. Analysis of the highest performance discharges with the EDGE2D/NIMBUS [31] codes shows [17] the higher Z_{eff} at the edge observed in the MkII divertor, compared to that in MkI, taking into account the change in the chemical sputtering yield with the different base temperatures of the MkI (40°C) and MkII (270°C) divertors.

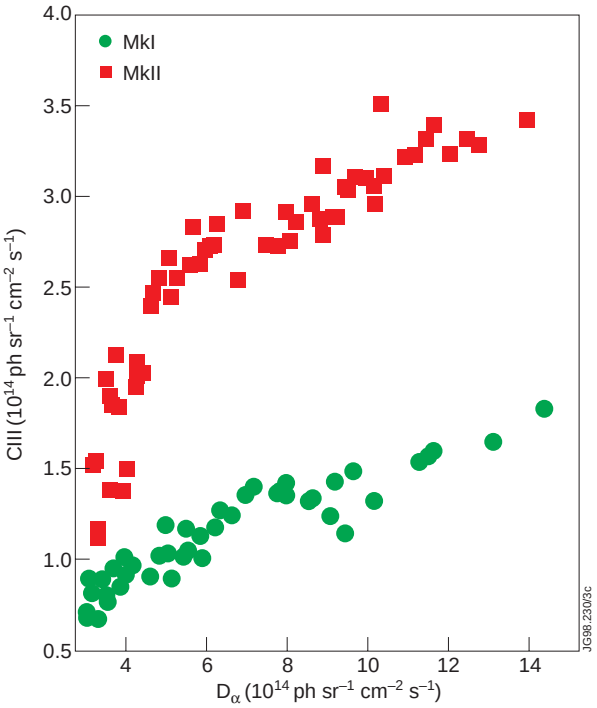

Fig. 10. CIII photon emission from the outer divertor as a function of the $D\alpha$ photon fluxes.

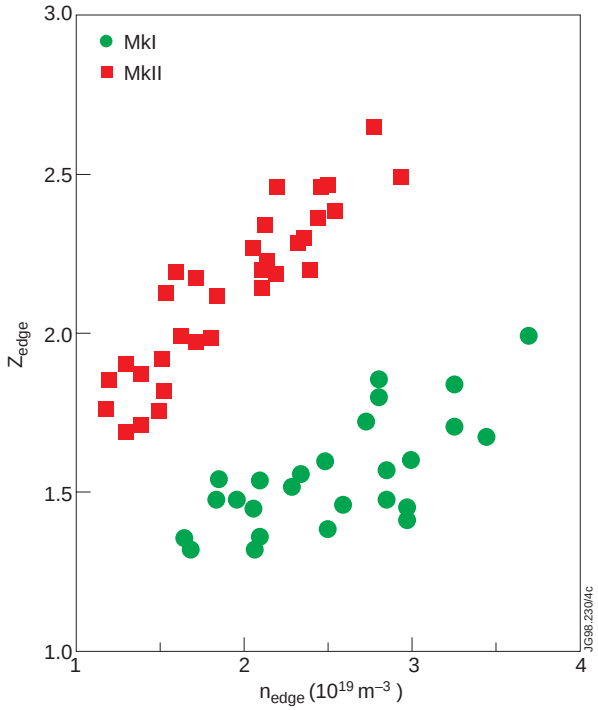

Fig. 11. Comparison of $Z_{eff,edge}$ between MkI and MkII.

A systematic increase in the power losses has been observed between MkI and MkII hot-ion H-modes. In particular, Fig. 12 compares the loss power and $Z_{eff,edge}$ for #40346 (MkII) with those for the MkI D-D hot-ion H-mode, #33643. Pulse 33643 delivered the highest fusion performance in the MkI campaign with similar NB heating power compared to the MkII pulse. As can be seen, the loss power in the MkII hot-ion mode is significantly higher, at a given edge density, than that in the MkI pulse, and correlates with a higher Z_{eff} at the edge.

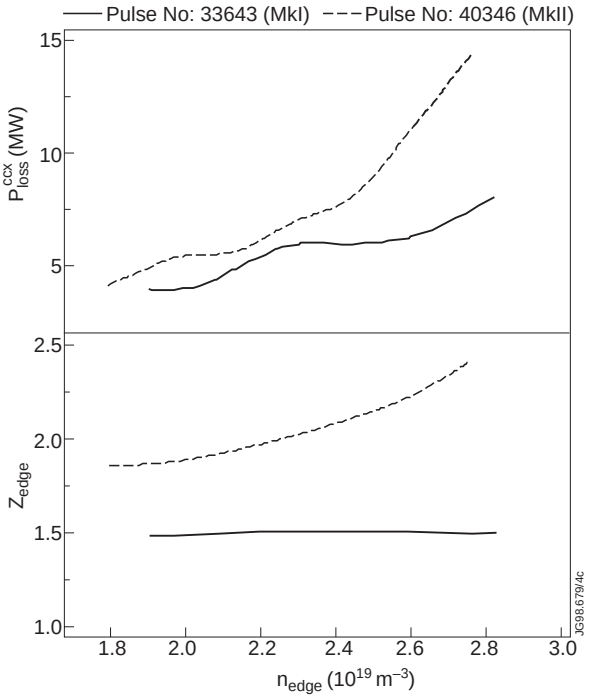

Fig. 12. Comparison of loss power and Z_{eff} at the edge between #40346 (MkII) and #33643 (MkI), which have similar NB heating (~20MW).

5.2 Effect of edge recycling

The rate of rise of the edge density is dependent on the recycling of neutrals from the main chamber and the divertor, in addition to the particle transport from the confined plasma core. It has been demonstrated in [3] that for hot-ion H-modes with the MkI divertor, the minimum recycling condition is essential for maximising the ELM-free period and improving the fusion performance. However, in going from MkI to the more closed MkII divertor the pressure of neutrals in the divertor increased by a factor of two and hence increase pumping. This strong divertor pumping has reduced the need for extensive conditioning for access to the hot-ion regime and increased the reproducibility of the performance achieved [4]. However, the plasma density rise during the ELM-free phase is reduced, as shown in Fig. 13, where the divertor neutral pressure and the edge density are compared between the discharges in MkI (#33643) and MkII (#38093) with similar NB particle source and gas fuelling. Consequently, additional gas fuelling has to be used to raise the central plasma density and reduce the beam shine through losses. In addition, it was found that the gas puff/bleed could reduce the Z_{eff},

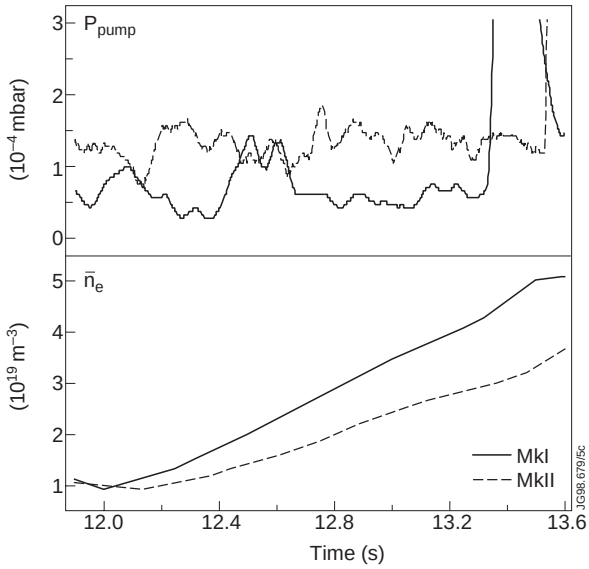

Fig. 13. Comparison of the neutral pressure in the subdivertor (and thus pumping speeds) and the density evolution for two ELM-free hot-ion H-modes in MkI (#33643) and MkII (#38093) divertors. The two discharges have similar NB particle sources and gas fuelling.

and delay the core MHD in some discharges [22]. However, inevitably, the gas fuelling also increases the edge density.

Apart from the higher Z_{eff} at the edge, as described in Section 5.1, the higher edge density is also responsible for the higher loss power observed in MkII. To illustrate this, we have selected the data close to the peak performance from the best of MkI and MkII NB and ICRF heated discharges, including both D-D and D-T hot-ion H-modes analysed by TRANSP. Fig. 14 plots the loss power, $P_{loss}{}^{ccx}$ computed by TRANSP as a function of the edge density. As can be seen, the loss power is clearly higher in MkII and is correlated with a higher edge density, except #38093 which has a lower edge density than the MkI discharge (#33643). Note that at similar edge densities, the loss power is also higher in MkII due to the higher Z_{eff}. A plot of $P_{loss}{}^{ccx}$ against $n_{edge}{}^{2} Z_{eff,edge} I_p{}^{-1} \sqrt{T_i / \langle E_{fast} \rangle}$ brings both the MkI and MkII data together and shows a good agreement with the neoclassical prediction, as illustrated in Fig. 15. This further confirms that the heat transport within the transport barrier is controlled by neoclassical transport processes and the loss power is dependent on the local plasma parameters at the edge transport barrier.

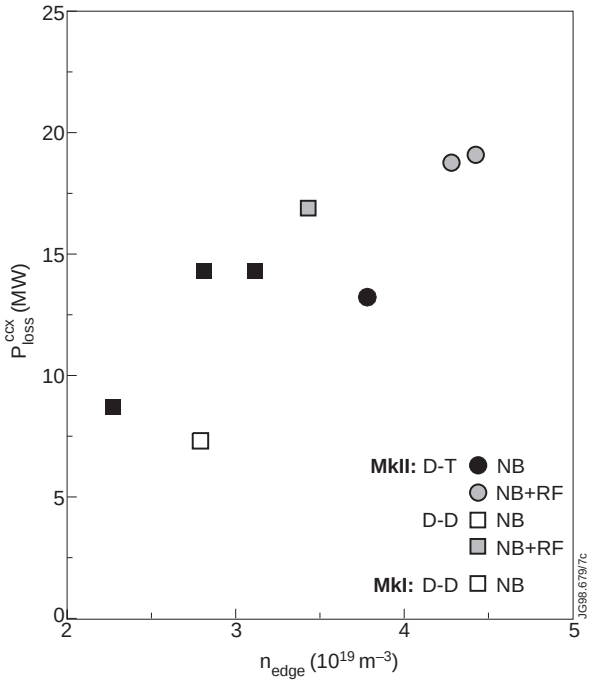

Fig. 14. $P_{loss}{}^{ccx}$ against n_{edge} for the high performance hot-ion H-modes from MkI and MkII. The data are taken close to the peak performance.

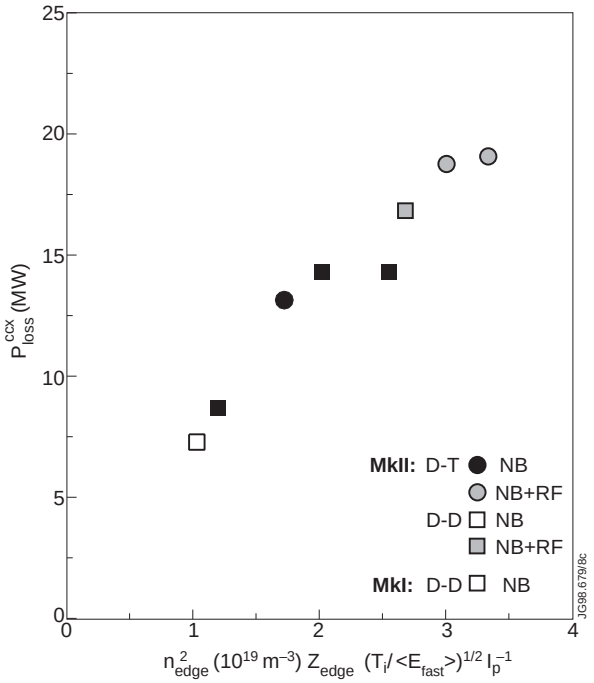

Fig. 15. $P_{loss}{}^{ccx}$ against n_{edge}^2 $Z_{eff,edge}$ $I_p{}^{-1}$ $\sqrt{T_i / \langle E_{fast} \rangle}$ for the high performance hot-ion H-modes from MkI and MkII.

It should be mentioned that Fig. 15 only shows a few of the best hot-ion discharges because TRANSP analysis can only be carried out for a limited number of cases. However, a survey of large numbers of hot-ion discharges using a rough estimation for the loss power ($P_{NBI} - P_{shine-through} - dW_{dia}/dt - P_{rad,core}$) supports the above findings [17].

6. SUMMARY AND CONCLUSIONS

Isotopic effects on the edge transport barrier have clearly been demonstrated for hot-ion H-modes on JET. D-T discharges have a higher edge pressure, immediately prior to the giant ELM which terminates the high performance phase, than seen in D-D hot-ion H-modes. The edge pressure increases more rapidly in D-T, due to additional heating from alpha particles, so resulting in an ELM-free period similar to that in the D-D cases.

The role of the fast particles has been elucidated by hot-ion H-mode discharges where the fast tritium particles are injected into the deuterium background plasma. These discharges attained a similar level of edge pressures, just prior to the terminating giant ELM, as tritium-rich discharges, except for a case with low tritium beam composition (25%). This suggests that a sufficient concentration of fast particles at the edge could affect the transport barrier. Additional evidence comes from pure deuterium discharges with differing fast particle energy. Higher edge pressure and longer ELM-free periods are produced with higher deuterium fast particle energy. Scaling for the width of the transport barrier shows that the best agreement with the experimental data is obtained assuming that the edge transport barrier width is given by a banana width of the fast particles.

Data from the hot-ion H-modes from both the MkI and the MkII divertor campaign show that loss power through the edge transport barrier scales as: $P_{loss} \propto n_{edge}{}^{2} Z_{eff,edge} I_p{}^{-1} \sqrt{T_i / \langle E_{fast} \rangle}$, as predicted by the neoclassical theory based on the width scaling of the fast particles. The carbon sources from the MkII divertor are about a factor of 2 higher than those in the MkI divertor. This results in a significant increase in Z_{eff} at the edge in MkII for the hot-ion H-modes, where the divertor shielding for impurities is poor, leading to the higher loss power in MkII. In addition, with the more closed MkII divertor, the divertor pumping for the recycling neutrals is strong and the central plasma density rise is slow so that additional gas fuelling is necessary to optimise the fusion performance. However, the gas fuelling also increases the edge plasma density, thus aggravating the power losses in MkII.

ACKNOWLEDGEMENTS

It is a pleasure to acknowledge the contributions from the rest of the JET staff. In particular, the authors gratefully acknowledge discussions and support from J. Lingertat, R.D. Monk, G.M. McCracken, P.C. Stangeby and G.Vlases.

REFERENCES

[1] M. Keilhacker et al., “High Fusion Performance from Deuterium-Tritium Plasmas in JET”, accepted by Nucl. Fusion (1998).

[2] P. Thomas et al., Phys. Rev. Lett. 80 (1998) 5548.

[3] P.J. Lomas (for the JET Team) in Proc. 15th IAEA Conf. on Fusion Energy, Seville, 1994, Vol. 1, p. 211.

[4] P.J. Lomas (for the JET Team), Proc. 16th IAEA Conf. on Fusion Energy, Montreal, 1996, Vol. 1, p. 239.
[5] V.V. Parail et al, in Proc. 15th IAEA Conf. on Fusion Energy, Seville, 1994, Vol. 1, p. 255.
[6] Cherubini et al., Plasma Phys. and Contr. Fusion 38 (1996) 1421.
[7] K.C. Shaing, and E.C. Crume, Jr. Phys. Rev. Lett. 63 (1989) 2369.
[8] P.H. Diamond and Y.B. Kim, Phys. Fluids B3 (1991) 1626.
[9] F. Romanelli and f. Zonco, Phys. Fluids B5 (1993) 4081.
[10] J. Lingertat et al., 24th EPS Conf. on Plasma Phys. and Contr. Fusion, Berchtesgaden, 1997, Or01; see also M. Keilhacker and the JET Team, Plasma Phys. and Contr. Fusion 39 (1997)B1.
[11] J.W. Connor and H.R. Wilson, UKAEA Fusion, Plasma Physics Note 97/4.1.
[12] B. Coppi, S.Migeiuolo et al., Phys. Fluids B2 (1990) 927.
[13] O. Pogutse et al., in 24th EPS Conf. on Plasma Phys. and Contr. Fusion, Berchtesgaden, 1997, Vol. 21A, Part III, p1041.
[14] F. Porchelli and M.N. Rosenbluth, Plasma Phys. and Contr. Fusion 40 (1998) 481.
[15] F.L. Hinton and G.M. Staebler, Phys. Fluids 5 (1993) 1281.
[16] V.V. Parail, H.Y. Guo, J. Lingertat, “Fast Particles and the Edge Transport Barrier”, submitted to Nucl. Fusion (1998).
[17] H.Y. Guo et al., “The role of recycling and impurity production in JET hot-ion H-modes”, to appear in J. Nucl. Mater. (Proc. 13th Int. Conf. on Plasma-Surface Interactions in controlled fusion devices, San Diego, 1998.)
[18] G.T.A. Huysmans et al., Proc. 22nd EPS Conf. on Plasma Phys. and Contr. Fusion, Bournemouth, 1995, Vol. 19C, Part I, p. 201.
[19] M.F.F.Nave et al., Nucl. Fusion 37 (1997) 809.
[20] E. Doyle et al., Phys. Fluids B3 (1991) 2300.
[21] J.W. Connor, Plasma Phys. Contr. Fusion 40 (1998) 531.
[22] M.F.F. Nave et al., Proc. 24th EPS Conf. on Plasma Phys. and Contr. Fusion, Berchtesgaden, 1997, Vol. 21A, Part I, p.1.
[23] M G von Hellermann et al. in Diagnostics for Experimental Thermonuclear Fusion Reactors, edited by P E Stott, G Gorini and E Sindoni, Plenum Press, New York and London, 1996, p. 281.
[24] J. Lingertat, “The edge operational space in JET”, to appear in J. Nucl. Mater. (Proc. 13th Int. Conf. on Plasma-Surface Interactions in controlled fusion devices, San Diego, 1998.
[25] A. Taroni et. al., 16th IAEA Fusion Energy Conf., Montréal, Canada, IAEA-CN-64/D3-3 (1996).
[26] P. Breger, Proc. 24th EPS Conf. Contr. Fusion Plasma Phys. Berchtesgaden, Germany, 1997, Vol. 21A, Part I, p.69.
[27] J. Wesson, “Tokamaks”, Clarendon Press, Oxford, 1987

[28] H.Y. Guo, G.F. Matthews, G. Vlases et al., “Effect of Chemical Sputtering in JET”, to be submitted to Nucl. Fusion.
[29] G.F. Matthews et al., J. Nucl. Mater. 196-198 (1992) 374.
[30] G.M. McCracken et al., “Studies in JET divertors of varied geometry III: intrinsic impurity behaviour”, accepted by Nucl. Fusion (1998).
[31] R. Simonini et al., Contrib. Plasma Phys. 34 (1994)368.